Agricultural and Forest Meteorology 202 (2015) 112–124

Contents lists available at ScienceDirect

Agricultural and Forest Meteorology

journal homepage: www.elsevier.com/locate/agrformet

Patterns of energy exchange for tropical ecosystems across a climate gradient in Mato Grosso, Brazil

Marcelo Sacardi Biudes[a,*], George Louis Vourlitis[b], Nadja Gomes Machado[a,c], Paulo Henrique Zanella de Arruda[a], Geraldo Aparecido Rodrigues Neves[a], Francisco de Almeida Lobo[a], Christopher Michael Usher Neale[d], José de Souza Nogueira[a]

[a] Programa de Pós-Graduação em Física Ambiental, Instituto de Física, Universidade Federal de Mato Grosso, Cuiabá, Mato Grosso, Brazil
[b] Biological Sciences Department, California State University, San Marcos, CA, USA
[c] Laboratório de Biologia da Convervação, Instituto Federal de Mato Grosso, Cuiabá, Mato Grosso, Brazil
[d] Civil and Environmental Engineering, Utah State University, Logan, UT, USA

ARTICLE INFO

Article history:
Received 8 April 2014
Received in revised form
17 December 2014
Accepted 18 December 2014

Keywords:
Amazon Basin
Climate change
Deforestation
Ecosystem function
Evapotranspiration
Sensible heat flux

ABSTRACT

The spatial and temporal variations in the partitioning of energy into latent (LE) and sensible (H) heat flux for tropical ecosystems are not yet fully understood. In the state of Mato Grosso State, Brazil, there are three different ecosystems (Cerrado, Pantanal and the Amazon Rainforest) with distributions that vary across rainfall and humidity gradients. Our goal was to analyze the seasonal variation in microclimate, spectral reflectance, LE and H for these ecosystems and quantify how energy partitioning varies across the regional climate gradient. We used the Bowen ratio energy balance method to estimate the LE and H of a dense, evergreen ombrophylous forest near Alta Floresta (AFL), a semi-deciduous forest in the Amazon-Cerrado transition zone near Sinop (SIN), a savanna grassland at Fazenda Miranda (FMI), a managed savanna pasture at Fazenda Experimental (FEX), a seasonally flooded woodland at Baía das Pedras in the Pantanal (BPE), and a riparian forest dominated by *Vochysia divergens* Pohl (CAM) in the Pantanal. Annual rainfall decreased from north to south, and 83% of the annual rainfall occurred during the wet season. However, the seasonal amplitude of volumetric soil water content (VSWC) increased from north to south, because of the increased potential for seasonal flooding. The vapor pressure deficit (VPD), air temperature, solar radiation (R_g) and net radiation (R_n) also increased from north to south, which directly affected the seasonal amplitude in the enhanced vegetation index (EVI). Our data suggest that energy partitioning in the wettest sites (AFL and CAM) were driven by solar radiation instead of soil water availability, while seasonal variation in rainfall was more important for the Amazon-Cerrado transitional forest (SIN), Cerrado (FMI and FEX) and Pantanal scrublands (BPE). These patterns are discernable using appropriate satellite vegetation indices, such as the EVI, allowing spatial and temporal variations in energy partitioning to be quantified across diverse landscapes like the Amazon Basin.

1. Introduction

Quantifying the partitioning of energy into latent (LE) and sensible (H) heat in the tropics, and its variation across landscapes, is critical for assessing hydrological cycles, understanding soil–plant–atmosphere interactions, and improving regional and global climate models. Energy partitioning varies between ecosystems due to interactions between biogeochemical cycling, plant physiology, soil water availability, and climate (Fisher et al., 2008; da Rocha et al., 2009; Costa et al., 2010). In Brazil, the distribution of land cover types is driven by climatic variations and anthropogenic influences, and in particular, the state of Mato Grosso has three different ecosystems, savanna (Cerrado), wetland (Pantanal) and Amazonian rainforest that are arrayed along broad climate gradients.

Although large regions of the Amazon Basin exhibit high annual rainfall there can be pronounced seasonality in rainfall and soil moisture due to the seasonal migration of Inter-Tropical Convergence Zone (ITCZ) (Machado et al., 2004; Marengo et al., 2011). Satellite measurements indicate that canopy greenness in the Amazon is negatively correlated with precipitation pattern (Saleska et al., 2003), with an increase in greenness and higher evapotranspiration and productivity during the dry season (Myneni et al., 2007; Huete et al., 2008) because productivity

* Corresponding author. Tel.: +55 65 3615 8738; fax: +55 65 3615 8738.
E-mail address: marcelo@fisica.ufmt.br (M.S. Biudes).

http://dx.doi.org/10.1016/j.agrformet.2014.12.008
0168-1923/

and evapotranspiration is limited more by radiation than water availability (Hutyra et al., 2007; Juárez et al., 2007; da Rocha et al., 2009). These patterns are opposite to those in more seasonal tropical ecosystems where dry season declines in precipitation create a water deficit that causes declines in evapotranspiration and productivity (Werth and Avissar, 2004; Giambelluca et al., 2009; Vourlitis et al., 2008, 2014; Costa et al., 2010; Rodrigues et al., 2014).

High spatial heterogeneity and climate–land surface interactions make patterns of tropical energy partitioning uncertain (Hasler and Avissar, 2007; Costa et al., 2010; Rodrigues et al., 2014). Such high spatial and temporal variation are particularly striking in the state of Mato Grosso, where three major ecosystems, Amazon forest, savanna (Cerrado), and wetlands (Pantanal), vary along climate gradients that vary in space and time. Moreover, within these regional ecosystems are landforms that vary substantially in physiognomy, due to a variety of variables such as soil type and fertility and exposure to seasonal flooding (Lopes and Cox, 1977; Furley and Ratter, 1988; Nunes da Cunha and Junk, 2004; Vourlitis et al., 2013). These ecosystems have experienced significant deforestation over the last several decades (Carvalho et al., 2009), and Mato Grosso has the dubious distinction of having some of the highest rates of deforestation in Brazil (Fearnside, 2003; Soares-Filho et al., 2006). Thus, within the state there is a mosaic of natural and managed forests, woodlands, plantations, croplands and pastures (Jasinski et al., 2005), which have widely varying hydrology and/or climate seasonality.

These spatial variations in hydrology and vegetation type alter the pattern of partitioning between LE and H, which feeds back on regional and global climate by affecting atmospheric humidity, thermal stability of the boundary layer, and regional precipitation (Hasler and Avissar, 2007; Costa and Pires, 2010). Deforestation can cause a decrease in evapotranspiration due to an increase in albedo, a decrease in surface roughness, and a decline in leaf area index (von Randow et al., 2004; Sheil and Murdiyarso, 2009). In turn, a decrease in evapotranspiration is typically linked with an increase in surface temperature, which acts to increase H (Biudes et al., 2012; Dubreuil et al., 2012). The ratio of LE/H may vary little above an intact forest, while above managed ecosystems, especially grass-dominated pastures and savanna, these fluxes have high variability throughout the year (Priante-Filho et al., 2004; Fisher et al., 2008; Biudes et al., 2009; Rodrigues et al., 2014). In turn, areas with higher H also have a convective boundary layer that can be up to 500 m higher than over intact forest (Fisch et al., 2004). The shift in the surface energy balance can influence regional, and potentially global, circulation and hydrology depending on the scale of the deforestation (Snyder, 2010; Bagley et al., 2014).

The high natural and anthropogenic variations in land cover type and climate highlight the need to understand seasonal and spatial variability of partitioning between LE and H. Here we exploit the high spatial and temporal variation of Amazon forest, Cerrado, and the Pantanal in the state of Mato Grosso to analyze the seasonal variation in microclimate, spectral reflectance, and LE and H in the dominant landforms of tropical Brazil. We hypothesize that (1) the seasonal amplitude of micrometeorology, spectral reflectance, and LE and H flux will increase from Amazon to Pantanal, and (2) the seasonality in LE and H will be driven by seasonal variation in precipitation and soil water content in all sites.

2. Materials and methods

2.1. Site descriptions

This study was conducted in six different ecosystems located across Mato Grosso, Brazil, two that were located within Amazon rainforest, two in the Cerrado and two in the Pantanal (Fig. 1). The periods in which data were available can be found in Table 1. The northernmost site was in a dense, evergreen ombrophilous forest located 39 km NE of the city of Alta Floresta (AFL) in the southern Amazon Basin (9°36′2.83″ S:55°55′22.22″ W). The vegetation is composed of *Tetragastris altissima* (22%), *Celtis schippii* (17%) and *Pseudolmedia* sp. (6%), with an average canopy height of 30 m but with some emergent trees reaching up to 45 m in height (Santos, 2005). The 30-year mean annual temperature in the Alta Floresta region is 25.7 °C, and rainfall is approximately 2230 mm year^{-1} with a dry season from June to September (Dubreuil et al., 2012). The soil is classified as a Vetic Acrisol (Hyperdystric), and it is acidic (pH = 4.5) with low level in phosphorus, extractable cation, and organic matter content (Quesada et al., 2010).

Further south, the next experimental area was in a dense, semi-deciduous forest located in the Amazon-Cerrado transition zone 50 km NE near the city of Sinop (SIN) (11°24′44.28″ S: 55°19′28.77″ W). Mean canopy height is 22–25 m, and leaf area index (LAI) varies between 2.5 m^2 m^{-2} during the dry season and approximately 6.0 m^2 m^{-2} during the wet season (Biudes et al., 2014a), and the vegetation is dominated by the tree species *Brosimum lactescens*, *Qualea paraensis* and *Tovomita schomburkii*

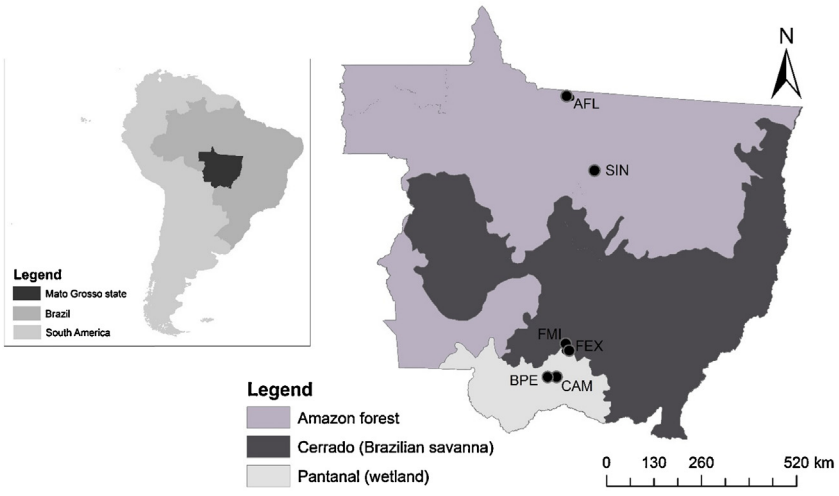

Fig. 1. Location of Mato Grosso, Brazil flux towers in a dense, evergreen ombrophylous forest at Alta Floresta (AFL), semi-deciduous transitional forest at Sinop (SIN), savanna mixed grassland-woodland (*campo sujo*) at Fazenda Miranda (FMI), *Brachiaria humidicola* pasture at Fazenda Experimental (FEX), seasonally flooded woodland at the Baía das Pedras (BPE) and the *Vochysia divergens* riparian forest (CAM) in the Pantanal.

Table 1
Overview flux tower sites and data availability in the state of Mato Grosso, Brazil.

Code	Locale	Ecosystem type	Years										
			03	04	05	06	07	08	09	10	11	12	13
AFL	Alta Floresta	Ombrophylous forest	X	X									
SIN	Sinop	Transitional forest (Cerradão)			X	X	X	X					
FMI	Fazenda Miranda	Savanna grassland (Campo sujo)							X	X	X	X	X
FEX	Fazenda Experimental	Non-native grassland				X	X	X	X	X			
BPE	Baía das Pedras	Seasonally flooded woodland									X	X	X
CAM	Cambarazal	Seasonally flooded forest				X	X	X	X	X			

(Vourlitis et al., 2014). The 30-year mean annual temperature in the Sinop area is 24 °C with little seasonal variation, and rainfall is approximately 2000 mm year^{-1} (Vourlitis et al., 2008) with a 4- to 5-month dry season (May–September). The soil is a Quartzarenic Neosol characterized by sandy texture (84% sand, 4% silt, and 12% clay) in the upper 50 cm of soil (Priante-Filho et al., 2004). The soils are poor in nutrients, have high porosity, and drain rapidly after rainfall events (Vourlitis et al., 2002).

Two sites were located within the Cerrado region that is south of the Amazon Basin (Fig. 1). One of the sites was in a mixed woodland–grassland (locally known as *campo sujo*) located at the Fazenda Miranda (FMI), which is 15 km S of the city of Cuiabá (15°43′53.66″ S: 56°04′18.81″ W). Vegetation is dominated by both native and non-native grasses and by the semi-deciduous tree species *Curatella americana* L. and *Diospyros hispida* A.DC. (Vourlitis et al., 2013). Nearby, another study site was in a non-native grassland located at the Fazenda Experimental (FEX), 33 km S of Cuiabá (15°51′15.23″ S: 56°04′13.50″ W). The pasture at FEX is dominated by the non-native *Brachiaria humidicola* (Biudes et al., 2008, 2009; 2012). The regional soil type is at both research sites is rocky, dystrophic red-yellow Latosol, also known as a Plinthosol (Radambrasil, 1982), with high rates of water infiltration but limited water holding capacity (Domingues et al., 2013). Mean annual rainfall and temperature of region are 1200 mm and 25.7 °C, respectively, and rainfall is seasonal with a dry season extending from May to September (Biudes et al., 2012).

The southernmost research sites were located in the Pantanal (Fig. 1), which is a 150,000 km^2 seasonally wetland that spans portions of Brazil, Paraguay, and Bolivia and is the largest wetland in the world (Nunes da Cunha and Junk, 2004). One research site was in a 3 m-tall seasonally flooded woodland located 105 km SW of Cuiabá (16°29′53.52″ S: 56°24′46.23″ W) at the Baía das Pedras Experimental Area (BPE). Vegetation consisted mainly of *Combretum laxum*, locally known as "pombeiro," which is a small tree/large shrub that grows in very dense thickets throughout the Pantanal (Santos et al., 2006). The other Pantanal site was located in a 26–28 m-tall seasonal flooded forest located 107 km SW of Cuiabá (16°33′19.11″ S: 56°17′11.49″ W). The vegetation is composed mainly of *Vochysia divergens* Pohl (Vochysiaceae), locally known as Cambarazal (CAM). Besides *V. divergens*, the vegetation is composed of *Duroia duckei* and *Ocotea longifolia* (Arieira and Nunes da Cunha, 2006). The leaf area index (LAI) of the CAM is 3.5 ± 0.2 m^2 m^{-2} with little seasonal variation (Biudes et al., 2014a). The topography of the floodplain is virtually flat, causing 1–2 m of flooding at both sites during the wet season (Nunes da Cunha and Junk, 2004). The soil is classified as a Gleyic Solonetz (Zeilhofer, 2006), and is acidic (pH = 4.7) with moderately high in phosphorus, cation, and organic matter content (Vourlitis et al., 2011; Machado et al., 2015). Annual rainfall and temperature of the region is on average 1400 mm and 26.1 °C with a pronounced dry season extending from May through September (Biudes et al., 2012, 2014a).

2.2. Micrometeorological measurements

A micrometeorological tower in each experimental area continuously collected data on solar radiation (R_g), net radiation (R_n), air temperature (T_a), relative humidity (RH), soil heat flux (G) and volumetric soil water content (VSWC). Sensors, data acquisition, and power supply systems are nearly identical at all sites, and a full list, including instrument model and installation information, is provided in Table 2. The manufacturers encourage calibrating the sensors every 2 years after field deployment; however, we calibrated all sensors every 6 months using a new instrument as reference in order to construct an accurate relationship between the outputs of each sensor.

2.3. Precipitation and enhanced vegetation index measurements

The precipitation data for each study site were obtained from the 3B43 V6 product of the Tropical Rainfall Measuring Mission (TRMM) satellite archived at the Distributed Active Archive System (DAAC) (http://disc2.nascom.nasa.gov/Giovanni/tovas/TRMM). The pixel size of TRMM is 25 km^2 (Danelichen et al., 2013).

We downloaded the 16-day MODIS Enhanced Vegetation Index (EVI) composites (Land Products Collection 5, MOD13Q1) from the Oak Ridge National Laboratory DAAC (http://daac.ornl.gov/cgi-bin/MODIS/GLBVIZ_1_Glb/modis_subset_order_global_col5.pl) based on the geo-location information (latitude and longitude) of each experimental area. The MOD13Q1 datasets include the EVI and Normalized Difference Vegetation Index (NDVI), at a spatial resolution of 250 m, and are corrected for the effects of atmospheric gases, aerosols, and thin cirrus clouds (Vermote and Kotchenova, 2008).

Table 2
Description of the equipment used to measure solar radiation (R_g), net radiation (R_n), air temperature (T_a) and relative humidity (RH), soil heat flux (G), soil water content (VSWC), and the respective height that each sensor was installed in each experimental area. Site abbreviations are as in Table 1.

Variable	Equipment description	Installed height (m)					
		FMI	FEX	BPE	CAM	SIN	AFL
R_g	LI200X, LI-COR, Lincoln, NE, USA	5	2	20	33	42	50
R_n	NRLITE, Kipp & Zonen, Delft, Netherlands	5	2	20	33	42	50
T_a/RH	HMP-45AC, Vaisala Inc., Woburn, MA, USA	5/18	0.5/1.8	22/31	33/37	39/45	45/51
G	HFP01, Hukseflux BV, Delft, The Netherlands	−0.01	−0.01	−0.01	−0.01	−0.01	−0.01
VSWC	CS-615, Campbell Sci., Logan, UT, USA	−0.2	−0.25	−0.2	0.25	0.25	0.25

2.4. Energy balance estimates by Bowen ratio method

Latent (LE) and sensible (H) heat flux and evapotranspiration (ET) estimates were calculated using the Bowen ratio energy balance method (BREB). The BREB method has been widely used since it was proposed in 1926 because it has the advantages of a clear physical concept, few parameter requirements, and a simple calculation method (Hu et al., 2013). The comparison of LE and H obtained with BREB method and eddy covariance method have shown that the BREB provides accurate and reliable values, and that instrument drifts on sub-annual time scales are minimal (Drexler et al., 2004; Biudes et al., 2009; Billesbach and Arkebauer, 2012; Dicken et al., 2013; Rodrigues et al., 2013). The BREB method we used followed the guidelines and modification described by Perez et al. (1999). Average fluxes of LE and H were calculated by Eqs. (1) and (2), respectively, at 30-min averaging intervals,

$$\mathrm{LE} = \frac{Rn - G - \Delta S}{1 + \beta} \quad (1)$$

$$\mathrm{H} = \frac{Rn - G - \Delta S}{1 + \beta^{-1}} \quad (2)$$

where LE and H is the latent and sensible heat flux ($\mathrm{W\,m^{-2}}$), R_n is the net radiation ($\mathrm{W\,m^{-2}}$), G is the ground heat flux ($\mathrm{W\,m^{-2}}$), and ΔS is the heat storage in the canopy air space and biomass calculated using the parameterization proposed by Moore and Fisch (1986). The ΔS was calculated every 30 min at AFL, SIN and CAM, but was negligible at FMI, FEX and BPE due to the low vegetation density. β is the Bowen ratio defined by Eq. (3),

$$\beta = \left(\frac{C_p}{\lambda 0.622}\right)\left(\frac{\Delta T}{\Delta e}\right) \quad (3)$$

where C_p is the specific heat at constant pressure ($1.00467\,\mathrm{J\,g^{-1}\,K^{-1}}$), 0.622 is the ratio of molecular weights of water and air, and ΔT and Δe are the difference of temperature (°C) and water vapor pressure (kPa) between the two measurement levels, respectively. The latent heat of vaporization (λ; $\mathrm{J\,g^{-1}}$) defined by Eq. (4)

$$\lambda = 1.919 \times 10^6 \left(\frac{T + 273.16}{(T + 273.16) - 33.91}\right)^2 \quad (4)$$

The average evapotranspiration ($\mathrm{mm\,30\text{-}min^{-1}}$) was calculated by Eq. (5),

$$\mathrm{ET} = \frac{\mathrm{LE}}{\lambda} \quad (5)$$

The daily evapotranspiration was obtained as the sum of 48 values of evapotranspiration at 30-min averaging intervals.

The criteria for accepting/rejecting data collected from the BREB method were based on those described by Perez et al. (1999) and revised by Hu et al. (2013). It was assumed that the gradients were sufficient in each experimental area due to the large fetches over relatively homogeneous terrain. The BREB method fails when (1) sensor resolution is inadequate to resolve gradients in ΔT and Δe (Unland et al., 1996), (2) stable atmospheric conditions, such as during the dawn and dusk, cause $\beta \approx -1$ (Ortega-Farias et al., 1996) and the evapotranspiration tends to infinity, and (3) conditions change abruptly leading to errors in measurement (Perez et al., 1999). Using this filtering method, physically realistic values of β can be obtained in an objective, quantitative manner, which limits the potential for bias and error in estimating energy balance terms (Perez et al., 1999; Hu et al., 2013).

2.5. Statistical analysis

EVI values were averaged for the nine pixels covering and surrounding the flux tower, and only pixels with highest quality assurance (QA) metrics were used. Varying sensor viewing geometry, cloud presence, aerosols and bidirectional reflectance can limit the efficacy of reflectance data for assessing spatial–temporal dynamics in biophysical processes (Hird and McDermid, 2009), and signal extraction techniques are often needed to improve the signal-noise ratio (Hernance et al., 2007). Thus, we applied Singular Spectrum Analysis (SSA) using the CatMV software (Golyandina and Osipova, 2007), which has been shown to be effective for the filtered reconstruction of short, irregularly spaced, and noisy time series and improving the signal-noise ratio of the MODIS EVI (Ghil et al., 2002).

Gaps in estimates of H and LE due to sensor failure and/or rejection of the Perez et al. (1999) criteria were filled by using linear relationships between retained values of LE and H as dependent variable and measured values of R_n–G as independent variable (see for example, Fig. 2) (Grace et al., 1996). The percentage of available energy (R_n) partitioned into LE and H was determined using linear regression with the origin forced through zero, where daily (24 h) average of LE or H (dependent variables) was regressed against daily R_n over monthly intervals (see for example, Fig. 3). The slope (±95% confidence interval) of these regressions indicates the relative partitioning of R_n into LE or H. The random errors associated with the averages of micrometeorological measurements and energy flux estimates were calculated as the ±95% confidence interval over monthly and annual intervals by bootstrapping the resampled time series over 1000 iterations (Efron and Tibshirani, 1993).

Links between the spatial variations in biophysical (EVI, LE, and H), hydrological (rainfall and VSWC), and meteorology (R_g, R_n, temperature, and VPD) variables between the study sites ($n = 6$) was assessed using linear correlation. Linear correlation was used because preliminary analyses indicated that linear models were superior to non-linear models for all variables considered. Analyses were conducted over seasonal (dry and wet) and annual intervals.

3. Results and discussion

3.1. Seasonal patterns of precipitation and soil water content

Total annual rainfall decreased from north to south from on average 2092 mm in the Amazon Basin (AFL and SIN) to 1496 in the Pantanal (BPE and CAM), and most of the annual rainfall (83%) was recorded during the months of October–March (Fig. 4 and Table 3). Rainfall for all sites reached a peak in January and decreased into May, which marked the beginning of the dry season (i.e., duration in which total monthly rainfall is <100 mm; Hutyra et al., 2007). Dry season duration was 4 months for AFL, 5 months for SIN, FEX, and FMI, and 6 months for the Pantanal study sites (Fig. 4). All sites exhibited a marked increase in rainfall in September, and rainfall increased during each month thereafter. These seasonal trends are consistent with the climatology for the region (Vourlitis and da Rocha, 2011; Biudes et al., 2012, 2014a).

Seasonal variations in volumetric soil water content (VSWC) tended to follow variations in rainfall, with highest values during the wet season and lowest values during the middle and end of the dry season (Fig. 4). For some sites, such as AFL, SIN, and FMI, the variations in soil water content were highly correlated with variations in rainfall; however, for the other sites, changes in soil water content tended to lag behind variations in rainfall. The lagged dynamics were especially pronounced in the Pantanal (BPE and CAM), because changes in soil water content are affected more by seasonal flooding dynamics than rainfall (Penha et al., 1999; Arieira and Nunes da Cunha, 2006; Biudes et al., 2009, 2014a). In general, the Pantanal sites had the highest average soil moisture of all of the other sites followed by the Amazonian forest and Cerrado sites

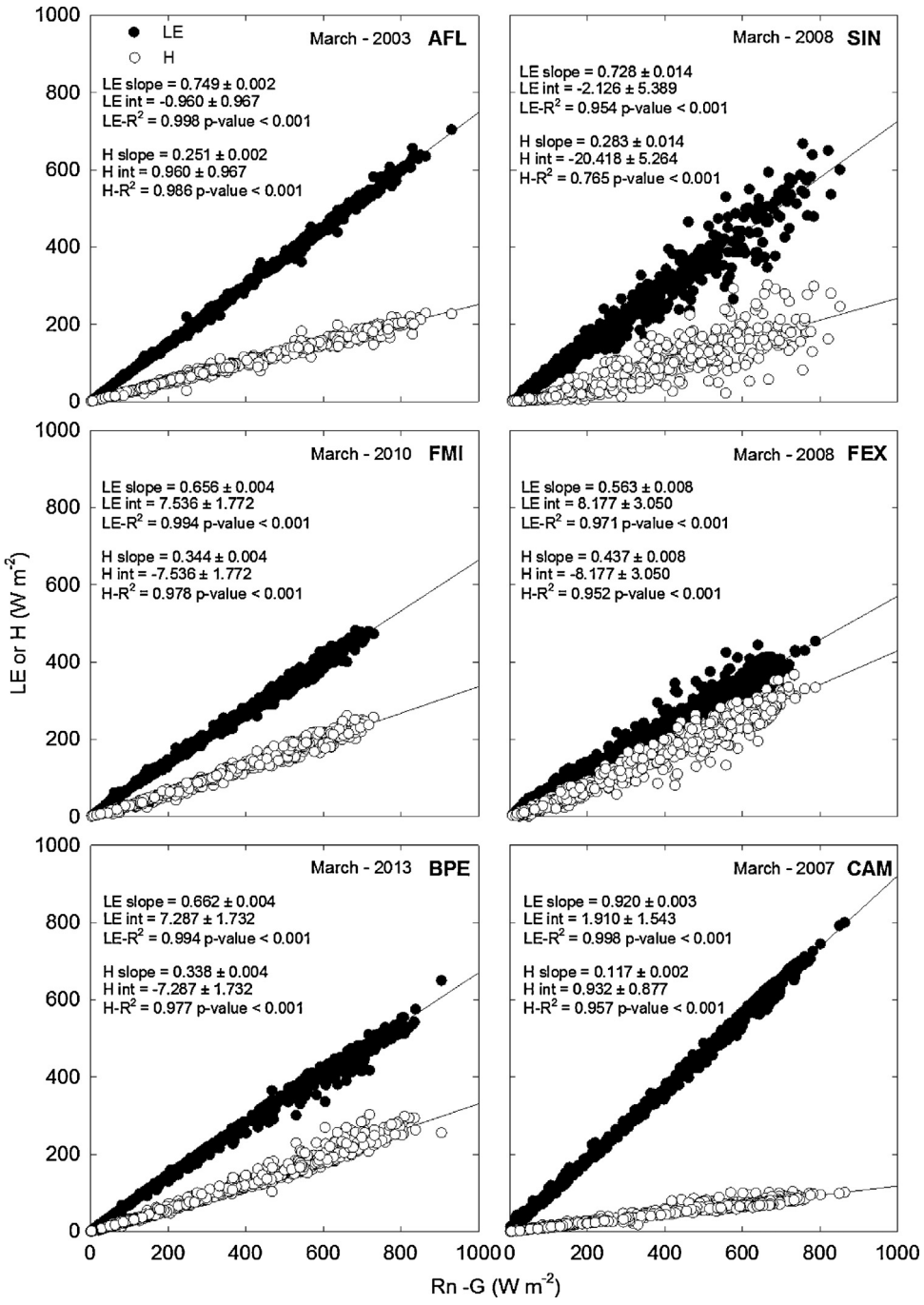

Fig. 2. An example of the linear regression method, slope (±95% confidence interval) and intercept (±95% confidence interval) of the equations used to fill the gaps in instantaneous (30-min average) latent heat flux (LE) and sensible heat flux (H) data sets obtained at the various research sites. Site abbreviations are as in Fig. 1.

(Fig. 4 and Table 3). In particular, FMI has the lowest soil moisture due to the sandy and rocky nature of the soil (Vourlitis et al., 2013), which has rapid rates of water infiltration but little water-holding capacity (Teepe et al., 2003).

3.2. Spatial and seasonal patterns of micrometeorological and spectral reflectance data

Average daily air temperature varied from 24 to 28 °C, but the seasonal amplitude (defined here as the difference between highest and lowest monthly average) for the Amazon Basin sites was considerably lower than the Cerrado and Pantanal sites (Fig. 5a). BPE was the coolest of these sites (minimum was 12.8 °C) and FMI the warmest (maximum was 33.2 °C). The largest annual temperature amplitude was observed at FMI (18.9 °C) while the smallest was observed for AFL (6 °C). However, the seasonal amplitude in air temperature for AFL was opposite to that observed for the other study sites (Fig. 5a) because of the increase in incident solar radiation that occurs in response to the decline in cloud cover during the dry season (Fig. 5c; da Rocha et al., 2009). For the other sites the air temperature exhibited consistent seasonal trends (Fig. 5a), with lowest values in the dry season when cold air transported by fronts out of the south (friagens) can persist for several days (Grace et al., 1996; da Rocha et al., 2009; Biudes et al., 2012). The peak air temperature at all sites occurred in September and October, except CAM and AFL where the maximum was in March and August,

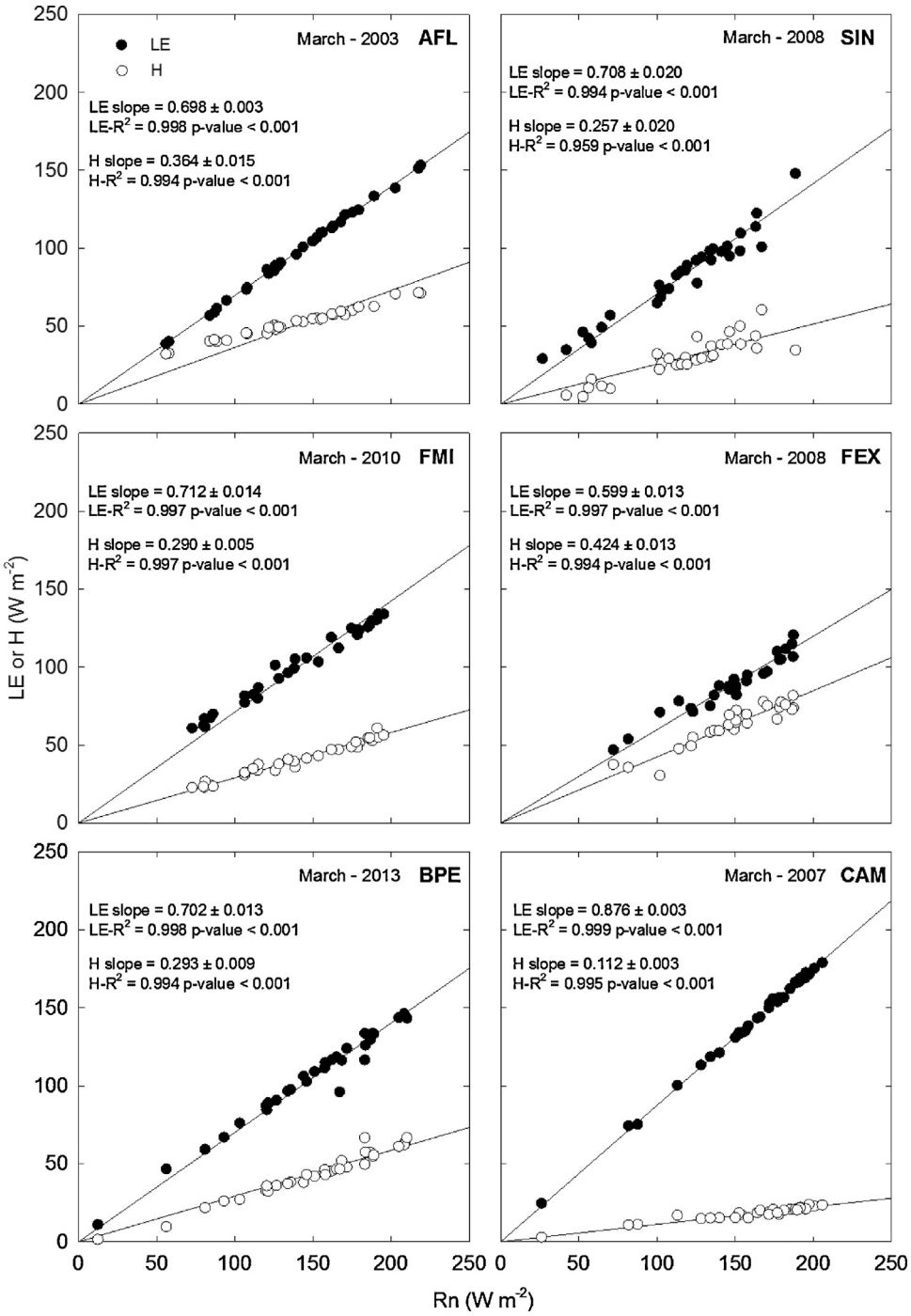

Fig. 3. An example of the linear regression method with the origin forced through zero and slope (±95% confidence interval) used to determine the percentage of daily available energy (R_n) partitioned into daily latent heat flux (LE) and daily sensible heat flux (H) obtained at the various research sites. Site abbreviations are as in Fig. 1.

respectively (Fig. 5a). The air temperature at SIN showed bimodal variation, with a minimum in early July around the solstice, and another minimum during December, coinciding with the maximum precipitation (Fig. 5a). The seasonal variation in VPD was opposite of that observed for rainfall, with higher values ranging 0.78–1.19 kPa recorded in the dry season (Fig. 5b). The peak of VPD was in July–August in the north and in September in the south, which is consistent with a variety of other tropical forests of the Amazon Basin (da Rocha et al., 2004; Vourlitis et al., 2014; Souza et al., 2014) and Pantanal (Biudes et al., 2014a).

The solar radiation (R_g) during the dry season increased at SIN and AFL but decreased at the other sites (Fig. 5c). In general, cloudiness ranging from 90% to 99% during the wet season causes a decline in incident solar radiation at low latitudes (Li et al., 1995; Hilker et al., 2012), and large cumulus or cumulonimbus clouds occasionally decrease the solar insolation reaching the surface to only 3% of that incoming at cloud top (Reynolds et al., 1975). On the other hand, biomass-burning aerosols can reduce the amount of incoming solar radiation to the land surface during dry season (Li et al., 2006), as was observed at FEX, FMI, CAM and BPE (Fig. 5c).

Forests had higher enhanced vegetation index (EVI) values than grasslands (Fig. 5d and Table 3), reflecting a higher leaf area index (LAI) associated with forest canopies (Ratana et al., 2005; Zhang et al., 2006). In general, the EVI was negatively correlated with the

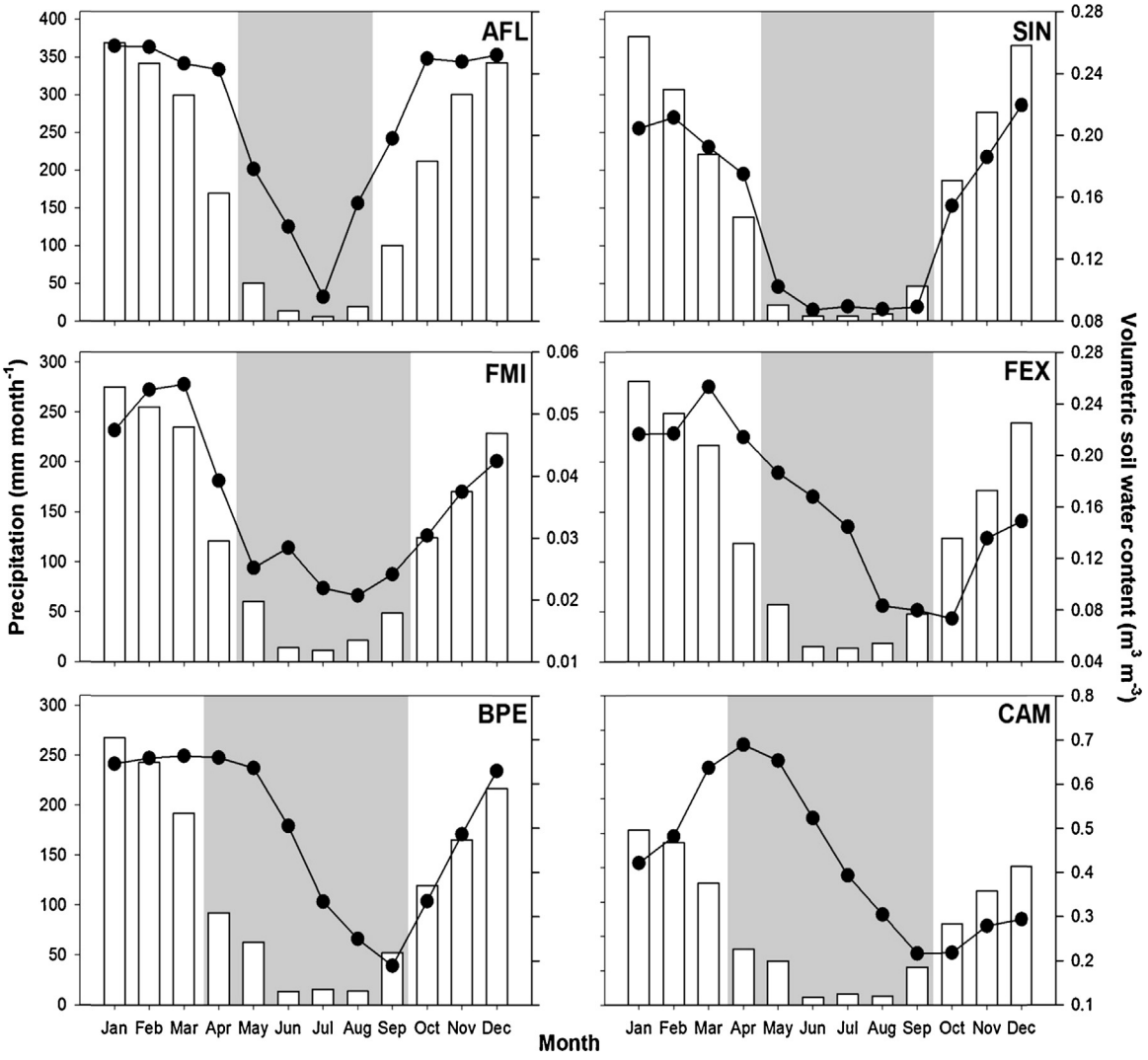

Fig. 4. Total monthly precipitation (open-bars; left-hand axis) and volumetric soil water content (solid circles and lines; right-hand axis) at the various research sites. The shaded portion in each figure depicts the dry season at each site. Site abbreviations are as in Fig. 1.

VPD and air temperature during the wet season and over the annual cycle (Table 4). Thus, warmer and sites with higher VPD tended to have lower EVI. Grasslands (FMI and FEX) and woodlands (BPE) also had higher seasonal variability in EVI than forests (Fig. 5d), which reflects the importance of dry season drought on LAI and canopy productivity (Ratana et al., 2005; Biudes et al., 2014a,b; Fausto et al., 2014). However, the minimum value for the EVI varied regionally, with the lowest values at the beginning of the dry season in the Amazon Basin and later in the dry season for the forests and woodlands of the Pantanal and the Cerrado grasslands (Fig. 5d). These lags in minimum greenness reflect the differing importance of radiation vs. water controls on LAI and productivity (Saleska et al., 2009), with

Table 3
Total annual rainfall (Ppt; mm) and mean (±95% Confidence Interval) annual volumetric soil water content (VSWC; $m^3\ m^{-3}$), vapor pressure deficit (VPD; kPa), air temperature (°C), solar radiation (R_g; $W\ m^{-2}$), Enhanced Vegetation Index (EVI), net radiation (R_n; $W\ m^{-2}$), latent heat flux (LE; $W\ m^{-2}$), sensible heat flux (H; $W\ m^{-2}$), and the ratio of net radiation dissipated by latent heat flux (LE/R_n) and sensible heat flux (H/R_n) in Amazonian forest (AFL and SIN), Cerrado (FMI and FEX), and Pantanal (BPE and CAM) ecosystems of Mato Grosso, Brazil.

Variable	Amazon forest		Cerrado		Pantanal	
	AFL	SIN	FMI	FEX	BPE	CAM
Ppt	2223	1962	1567	1553	1457	1395
VSWC	0.21 ± 0.03	0.15 ± 0.03	0.07 ± 0.02	0.16 ± 0.03	0.50 ± 0.10	0.43 ± 0.09
VPD	0.84 ± 0.19	0.63 ± 0.12	1.03 ± 0.23	0.99 ± 0.12	1.04 ± 0.22	0.87 ± 0.20
T	24.7 ± 0.3	24.5 ± 0.4	26.3 ± 0.9	26.5 ± 0.9	26.0 ± 0.8	26.1 ± 0.8
R_g	174.3 ± 7.5	171.5 ± 5.7	196.5 ± 7.2	160.8 ± 9.2	202.0 ± 10.4	203.2 ± 13.3
R_n	123.7 ± 7.5	127.5 ± 8.4	116.5 ± 11.5	121.9 ± 12.8	137.3 ± 9.7	119.1 ± 15.0
EVI	0.54 ± 0.02	0.53 ± 0.02	0.32 ± 0.03	0.36 ± 0.03	0.40 ± 0.04	0.46 ± 0.02
LE	85.1 ± 5.8	80.3 ± 7.2	70.8 ± 12.2	68.8 ± 8.9	88.6 ± 10.1	96.4 ± 12.0
H	34.7 ± 4.5	40.1 ± 5.3	41.2 ± 3.6	52.2 ± 4.0	48.6 ± 4.9	20.9 ± 4.4
LE/R_n	0.69 ± 0.01	0.63 ± 0.05	0.60 ± 0.06	0.56 ± 0.02	0.64 ± 0.04	0.81 ± 0.03
H/R_n	0.28 ± 0.03	0.32 ± 0.04	0.37 ± 0.05	0.44 ± 0.03	0.36 ± 0.04	0.18 ± 0.03

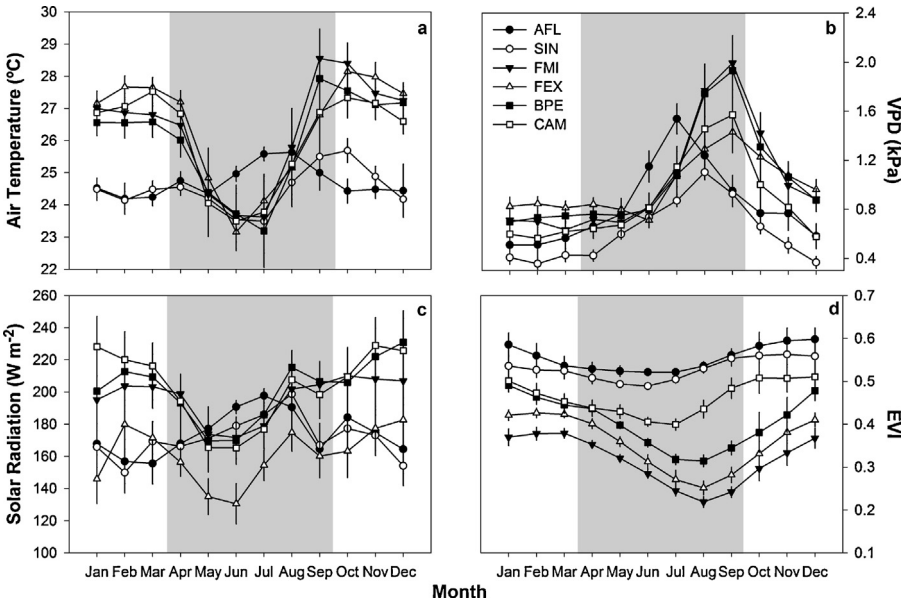

Fig. 5. Mean (±95% confidence interval) monthly (a) air temperature (°C), (b) vapor pressure deficit (VPD; kPa), (c) solar radiation (W m^{-2}), and (d) enhanced vegetation index (EVI) at AFL (solid-line; closed-circles), SIN (dotted-line; open-circles), FMI (short-dashed-line; inverted-closed-triangle), FEX (dot-dashed-line; open-triangle), BPE (long-dashed-line; closed-square) and CAM (dot-dashed-line; open-square) in the Pantanal. Site abbreviations are as in Fig. 1. The shaded portion in each figure depicts the approximate dry season for the study sites.

radiation being more important in the northern areas while seasonal drought being more important in the south (Machado et al., 2004; Biudes et al., 2014a,b). In general, all of the sites had higher values of the EVI during the wet season (Fig. 5d), which is in contrast to other studies in the Amazon Basin where canopy greenness was negatively correlated with precipitation (Saleska et al., 2003, 2009). However, the mechanism for the higher EVI values during dry season is still open to debate. Some suggest that the high dry season EVI values are an adaptation to an increase in solar radiation and/or avoidance of herbivory (Xiao et al., 2006) while others suggest it is an artifact due to the decrease in the solar zenith angle, and thus, an increase in illumination that occurs during the dry season (Galvão et al., 2011). Regardless, our data indicate that seasonal trends in rainfall, rather than radiation, are more important for the seasonal trend in the EVI for the research sites observed here.

3.3. Spatial and seasonal patterns in energy flux

Amazonian forests showed the smallest seasonal variations in net radiation (R_n), while the Cerrado grasslands and the Pantanal ecosystems had marked declines in R_n during the dry season, which were similar to that observed for R_g (Fig. 5c). The R_n is a function of the spectral characteristics of the surface (Rodrigues et al., 2009), and forests as AFL and SIN have lower surface albedo (11–14%) and higher moisture and LAI than grassland, absorbing more sunlight (Breuer et al., 2003). Furthermore, forests have higher biomass, observed by higher EVI (Fig. 5e), which reduces the canopy temperature and long wave canopy emission, and increases R_n (Santos et al., 2011). These properties tended to maintain higher R_n (and EVI) during the dry season, while during the wet season, prolonged cloud cover reduced the R_g, and consequentially R_n (da Rocha et al., 2009; Vourlitis et al., 2014). Thus, variations in R_n for the Amazonian forests were minimal compared to the southern ecosystems.

The R_n was typically higher during the wet season at FMI, FEX, BPE and CAM (Fig. 6), which is consistent with the seasonal variation in the solar angle and an increase in soil water availability in Cerrado (Rodrigues et al., 2013, 2014) and Pantanal (Biudes et al., 2009). In turn, declines in R_n in the Cerrado and Pantanal during dry season were due in part to an increase in the surface albedo caused by a decline in vegetation greenness and/or leaf area, which was also reflected in the lower dry season EVI (Machado et al., 2004; Ratana et al., 2005; Biudes et al., 2014a,b; Rodrigues et al., 2013; 2014). However, it is interesting to note that the Pantanal woodland BPE had the highest average annual R_n (Table 3) due to the dense nature and high LAI of the *Combretum* woodlands (Santos et al., 2006).

The latent heat flux (LE) values were higher than sensible heat flux (H) in all sites during the study period (Fig. 6 and Table 3). The highest LE values were observed in the Pantanal (CAM and BPE), followed by Amazon Forest (AFL and SIN) and Cerrado (FMI and

Table 4
Linear correlation coefficients for the Enhanced Vegetation Index (EVI), latent (LE) and sensible (H) heat flux, and the ratio of LE and H to net radiation (LE/R_n and H/R_n, respectively) as a function of the EVI, precipitation (Ppt), volumetric soil water content (VSWC), atmospheric vapor pressure deficit (VPD), air temperature (T), and solar (R_g) and net (R_n) radiation during the wet and dry seasons and annual time periods. Bold values are statistically significant ($p < 0.05$; $n = 6$ sites).

Variable	EVI			LE			H			LE/R_n			H/R_n		
	Dry	Wet	Ann	Dry	Wet	Ann	Dry	Wet	Ann	Dry	Wet	Ann	Dry	Wet	Ann
EVI	–	–	–	**0.88**	0.12	0.57	−0.26	−0.64	−0.48	0.49	0.65	0.61	−0.54	−0.66	−0.63
Ppt	0.21	0.71	0.71	0.24	−0.54	−0.08	−0.04	−0.36	−0.05	0.05	0.17	−0.04	−0.15	−0.27	−0.15
VSWC	0.10	0.30	0.16	0.51	0.74	**0.82**	−0.48	−0.02	−0.24	0.73	0.37	0.54	−0.58	−0.21	−0.38
VPD	−0.63	**−0.87**	**−0.83**	−0.26	−0.02	−0.23	−0.12	**0.81**	0.38	0.01	−0.67	−0.35	0.03	0.75	0.43
T	−0.68	**−0.86**	**−0.89**	−0.41	0.25	−0.23	−0.22	0.54	0.22	0.02	−0.42	−0.26	−0.02	0.49	0.33
R_g	0.19	−0.40	−0.23	0.40	**0.85**	0.58	−0.31	−0.12	−0.43	0.27	0.34	0.44	−0.30	−0.24	−0.38
R_n	0.63	−0.48	0.24	0.52	0.61	0.31	0.53	0.45	0.43	−0.20	−0.15	−0.11	0.21	0.30	0.25

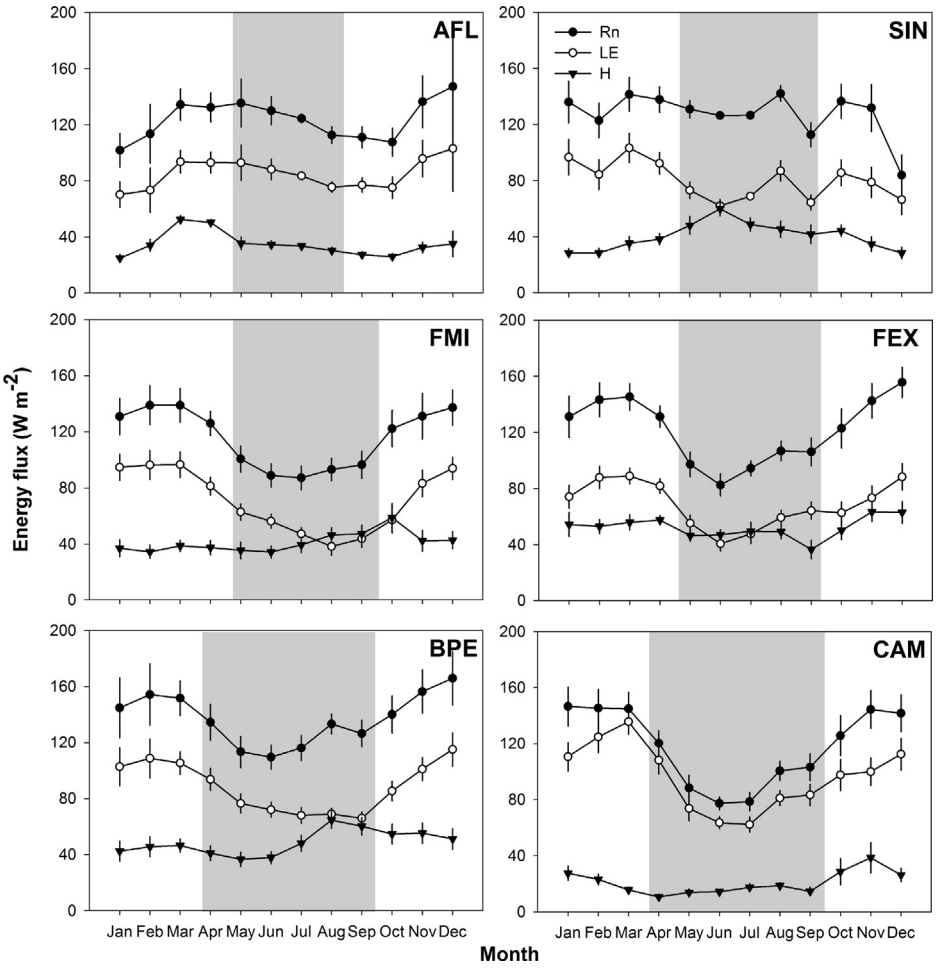

Fig. 6. Mean (±95% confidence interval) monthly net radiation (R_n; solid-line; closed-circles), latent heat flux (LE; dotted-line; open-circles) and sensible heat flux (H; dashed-line; inverted-closed-triangle) at the various research sites. The shaded portion in each figure depicts the dry season at each site. Site abbreviations are as in Fig. 1.

FEX). Spatial variations in LE were correlated with the EVI, VSWC, or R_g depending on the time interval of interest (Table 4). For example, dry season variations in LE were positively correlated with the EVI, thus areas with higher greenness and/or LAI had higher dry season rates of LE, a trend that is typical of the Amazon Basin as a whole (Rodrigues et al., 2014) and reflects higher and more consistent LAI (Ratana et al., 2005) and deeper rooting depth of trees that contribute to the high dry season EVI (Fisher et al., 2007). In contrast, spatial variations in LE during the wet season were positively correlated with solar radiation (R_g), which reflects the relatively greater energy limitation on LE when water limitation is negligible (da Rocha et al., 2009; Rodrigues et al., 2014). Finally, over annual time periods, LE was positively correlated with VSWC, reflecting the importance of water availability on LE (Malhi et al., 2008; da Rocha et al., 2009; Vourlitis et al., 2014). In contrast, the lowest H values occurred in high-density forests (AFL, SIN and CAM) while the higher H values occurred in the BPE and Cerrado grasslands (Fig. 6 and Table 3). Spatial variations in H were positively correlated with VPD during the wet season (Table 4), thus, forested areas that maintained high rates of evapotranspiration also had a lower air temperature and atmospheric water vapor demand, which increased LE but reduced H (Alves et al., 1999; Betts et al., 2008; Malhi et al., 2008).

Temporal variations in LE were smaller for the Amazonia forests than for the Cerrado grasslands and Pantanal woodlands (Fig. 6). LE was higher for FMI, FEX, CAM and BPE during the wet season, which is positively correlated with the seasonal trend in R_n and soil water availability. At all of the sites except AFL and CAM, rates of LE declined enough during the dry season that average monthly rates of H either equaled or exceeded LE, especially in the Cerrado grasslands. The drought stress due to low rainfall, soil water content, and/or water holding capacity of the savanna soils causes LE to decrease during the dry season (Giambelluca et al., 2009; Rodrigues et al., 2014); however, for riparian forests and forests of the Amazon Basin, dry season declines in LE are not as pronounced because closed tree canopies limit evaporation and deeply rooted trees have access to more consistent, deeper soil water reserves (Fisher et al., 2007).

3.4. Normalized energy fluxes and energy partitioning

The partitioning of R_n into LE and H affects the boundary layer development and the vertical transport of the heat and water vapor in the atmosphere, which ultimately influences regional and global cloud formation and precipitation (Dirmeyer, 1994; Seth and Giorgi, 1996; Pielke, 2001). The amount of R_n dissipated by LE (LE/R_n) and H (H/R_n) varied significantly between vegetation types and over time (Fig. 7 and Table 3); however, there were no statistically significant correlations between the spatial variations in LE/R_n or H/R_n and the meteorological drivers (Table 4). Between 69% and 81% of the R_n was partitioned into LE for AFL and CAM, with little seasonal variation (Fig. 7A and F). These tall, dense forests appear to be able to withstand the dry season without soil moisture restrictions on evapotranspiration (Biudes et al., 2009; Fisher et al., 2008). However, there may be fundamental differences in the mechanisms in which these forests are able to partition consistently

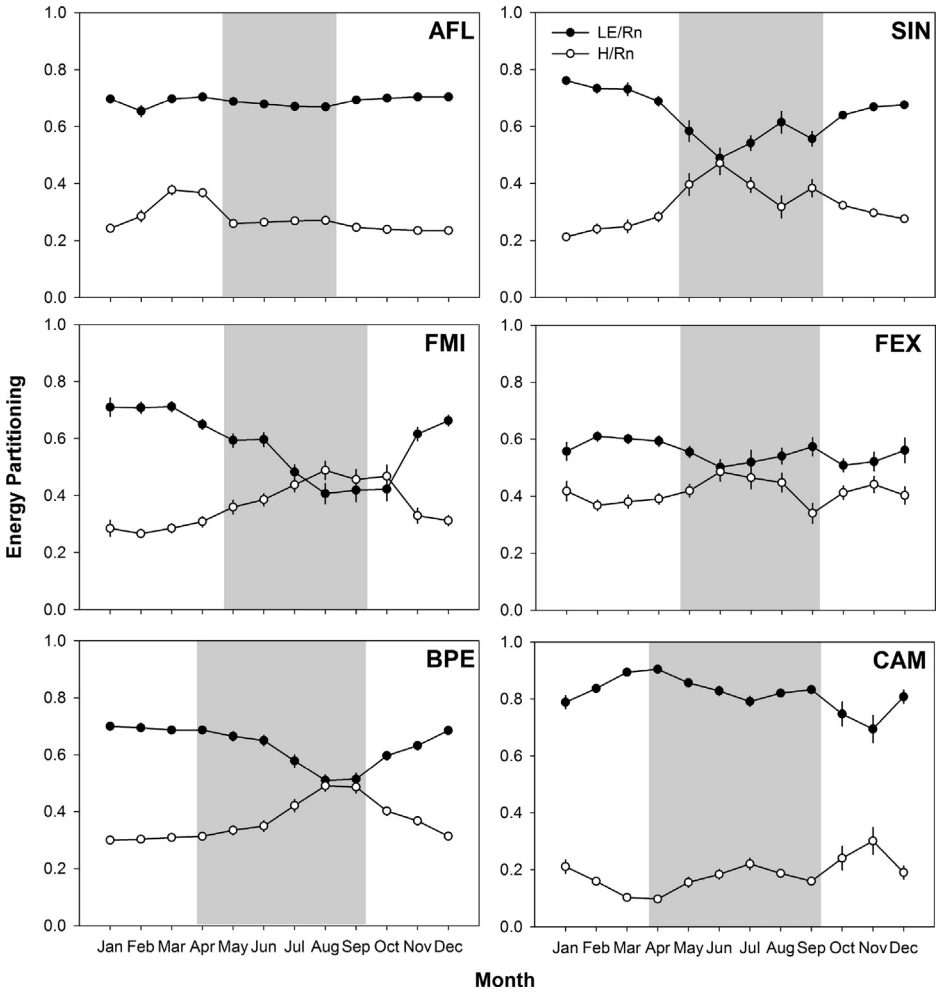

Fig. 7. Mean (±95% confidence interval) monthly of net radiation dissipated by latent heat flux (LE/R_n; solid-line; closed-circles) and sensible heat flux (H/R_n; dotted-line; open-circles) at the various research sites. The shaded portion in each figure depicts the dry season at each site. Site abbreviations are as in Fig. 1.

more R_n to LE during the annual cycle. The Amazon forest has an active root biomass profile which can extract water down to 5.0 m (Fisher et al., 2007), thus maintaining a high rate of transpiration during the dry season (Vourlitis et al., 2008). In contrast, the seasonally flooded forest has ample surface soil moisture during the dry season, which acts to maintain both high evaporation and transpiration of the dominant tree species, *Vochysia divergens*, throughout the dry season (Biudes et al., 2009; Dalmagro et al., 2014).

At the other sites, the amount of R_n partitioned into LE or H varied as a function of season. For SIN, FMI, and BPE, the amount of R_n partitioned into LE declined during the dry season months and either equaled (SIN and BPE) or was lower than (FMI) the amount of R_n partitioned into H (Fig. 7B, C, E). These patterns suggest that temporal trends in energy partitioning into LE in these four sites was limited by water availability (Giambelluca et al., 2009; Rodrigues et al., 2014; Vourlitis et al., 2008; 2014). Similar patterns were observed for the other Cerrado grassland (FEX); however, seasonal variations were much smaller compared to FMI. The relatively higher dry season partitioning of R_n into LE at FEX has been observed in similar pastures in (Priante-Filho et al., 2004; von Randow et al., 2004) and may reflect a higher resistance to water stress by African grasses, such as *B. humidicola*, compared to native savanna grasses (San Jose et al., 1998). There is also evidence that some *Brachiaria* grasses have roots as deep as 1.5 m, which allows them to access deeper soil water during the dry season (Santos et al., 2004).

4. Conclusions

We hypothesized that the seasonal amplitude of micrometeorology, spectral reflectance, and LE and H flux would increase from the Amazon Basin to the Pantanal in the state of Mato Grosso and that the seasonality in LE and H would be driven by seasonal variation in precipitation and soil water content. We found that seasonal variations in precipitation and soil water content were not important for energy partitioning in the mature rainforest (AFL) and the seasonal flooded forest (CAM) because these forests were limited more by radiation than by water. Water limitations were more important in controlling seasonal variations in H and LE for the transitional forest (SIN), Cerrado grassland and woodland (FMI and FEX), and the seasonally flooded Pantanal woodland (BPE), where the prolonged dry season led to seasonal drought. However, spatial variations in LE were not driven by precipitation. Rather, spatial variations in H and LE varied by season, with LE being positively correlated with spectral reflectance (EVI) during the dry season, because forests with higher leaf area had higher transpiration, and positively correlated with solar radiation in the wet season, because forests with lower cloud cover had more energy for evapotranspiration. These spatial and temporal variations lead to a complex pattern of energy partitioning, where energy fluxes are affected by both surface (leaf area, soil water content) and meteorological (precipitation, radiation) feedbacks. In turn, these feedbacks affect surface temperature and humidity, boundary

layer development, cloud formation, and thus, local and regional climate.

Our results also have implications for land cover change, which has been widespread through the state of Mato Grosso (Jasinski et al., 2005), and is expected to increase over the next 3–4 decades (Soares-Filho et al., 2006). Climate models predict that the dry season is likely to increase in duration and/or intensity (Li et al., 2006; Costa and Pires, 2010). If so, then our data suggests that declines in both soil water content and leaf area will result in lower evapotranspiration, higher surface temperature, and a shift in the partitioning of radiation from LE to H. A change in energy partitioning toward H would reduce cloud cover and rainfall, which could further reduce tree cover and leaf area and enhance local and regional warming. Higher temperatures over deforested surfaces can enhance convection, which can draw moist air from forested surfaces (Baidya Roy and Avissar, 2002; Garcia-Carreras and Parker, 2011). Over time, localized warming and drying can reduce E of forest fragments (Pongratz et al., 2006; Costa and Pires, 2010). Such a scenario is consistent with some, but not all, climate model simulations (Werth and Avissar, 2002; Li et al., 2006) and recent observations (Malhi and Wright, 2005; Li et al., 2008; Vourlitis et al., 2014).

Acknowledgments

The research was supported in part by the Universidade Federal de Mato Grosso (UFMT), Programa de Pós Graduação em Física Ambiental (PPGFA) IF/UFMT, Coordenação de Aperfeiçoamento de Pessoal do Ensino Superior (bolsistas CAPES Proc. n° 9750/13-4 e 9768/13-0), Conselho Nacional de Desenvolvimento Científico e Tecnológico (MCT-CNPq-CT Infra-CT Energia n° 07/2006; Code: 620082/2006-2), Fundação de Amparo à Pesquisa do Estado de Mato Grosso (PRONEX/FAPEMAT – 2009 – Code: 823971/2009; Edital Universal/FAPEMAT 005/2012 – Proc. n° 331763/2012; PRONEN/FAPEMAT 008/2014 - Proc. n° 561397/2014), the National Geographic Society, Committee for Research and Exploration, the National Science Foundation, Division of International Programs (OISE-0003778; IRES-0968245), and Division of Environmental Biology-Ecosystem Studies (DEB-0343964).

References

Alves, F.S.M., Fisch, G., Vendrame, I.F., 1999. Modificações do microclima e regime hidrológico devido ao desmatamento na Amazônia: um estudo de caso em Rondônia (RO), Brasil. Acta Amazônica 29 (3), 395–409.

Arieira, J., Nunes da Cunha, C., 2006. Fitossociologia de uma floresta inundável monodominante de *Vochysia divergens* Pohl (Vochysiaceae), no Pantanal Norte, MT, Brasil. Acta Bot. Bras. 20 (3), 569–580, http://dx.doi.org/10.1590/S0102-33062006000300007.

Bagley, J.E., Desai, A.R., Harding, K.J., Snyder, P.K., Foley, J., 2014. Drought and deforestation: has land cover change influenced recent precipitation extremes in the Amazon? J. Clim. 27, 345–361, http://dx.doi.org/10.1175/JCLI-D-12-00369.1.

Baidya Roy, S., Avissar, R., 2002. Impact of land use/land cover change on regional hydrometeorology in Amazonia. J. Geophys. Res. Atmos. 107, http://dx.doi.org/10.1029/2000JD000266.

Betts, R., Sanderson, M., Woodward, S., 2008. Effect of large-scale Amazon forest degradation on climate and air quality through fluxes of carbon dioxide, water, energy, mineral dust and isoprene. Philos. Trans. R. Soc. B 363, 1873–1880, http://dx.doi.org/10.1098/rstb.2007.0027.

Billesbach, D.P., Arkebauer, T.J., 2012. First long-term, direct measurements of evapotranspiration and surface water balance in the Nebraska Sand-Hills. Agric. For. Meteorol. 156, 104–110, http://dx.doi.org/10.1016/j.agrformet.2012.01.001.

Biudes, M.S., Valentini, C.M.A., Campelo-Júnior, J.H., Nogueira, J.S., 2008. Estimativa da evapotranspiração numa pastagem mista, em condições de Cerrado, pelos métodos de razão de Bowen e Penman-Monteith. Ciência e Natura 30 (1), 71–86.

Biudes, M.S., Campelo Júnior, J.H., Nogueira, J.S., Sanches, L., 2009. Estimativa do balanço de energia em cambarazal e pastagem no norte do Pantanal pelo método da razão de Bowen. Rev. Bras. Meteorol. 24 (2), 135–143, http://dx.doi.org/10.1590/S0102-77862009000200003.

Biudes, M.S., Machado, N.G., Danelichen, V.H.M., Souza, M.C., Vourlitis, G.L., Nogueira, J.S., 2014a. Ground and remote sensing-based measurements of leaf area index in a transitional forest and seasonal flooded forest in Brazil. Int. J. Biometeorol. 58, 1181–1193, http://dx.doi.org/10.1007/s00484-013-0713-4.

Biudes, M.S., Nogueira, J.S., Dalmagro, H.J., Machado, N.G., Danelichen, V.H.M., Souza, M.C., 2012. Mudança no microclima provocada pela conversão de uma floresta de cambará em pastagem no norte do Pantanal. Revista de Ciências Agro-Ambientais 10, 61–68.

Biudes, M.S., Souza, M.C., Machado, N.G., Danellichen, V.H.M., Vourlitis, G.L., Nogueira, J.S., 2014b. Modelling gross primary production of a tropical semi-deciduous forest in the southern Amazon Basin. Int. J. Remote Sens. 35 (4), 1540–1562, http://dx.doi.org/10.1080/01431161.2013. 878059.

Breuer, L., Eckhardt, K., Frede, H.G., 2003. Plant parameter values for models in temperate climates. Ecol. Model. 169 (2/3), 237–293, http://dx.doi.org/10.1016/S0304-3800(03)00274-6.

Carvalho, F.M.V., de Marco Jr., P., Ferreira, L.G., 2009. The Cerrado intro-pieces: habitat fragmentation as a function of landscape use in the savannas of central Brazil. Biol. Conserv. 142, 1392–1403, http://dx.doi.org/10.1016/j.biocon.2009.01.031.

Costa, M.H., Biajoli, M.C., Sanches, L., Malhado, A.C.M., Hutyra, L.R., da Rocha, H.R., Aguiar, R.G., de Araújo, A.C., 2010. Atmospheric versus vegetation controls of Amazonian tropical rain forest evapotranspiration: are the wet and seasonally dry rain forests any different? J. Geophys. Res. 115, G04021, http://dx.doi.org/10.1029/2009JG001179.

Costa, M.H., Pires, G.F., 2010. Effects of Amazon and Central Brazil deforestation scenarios on the duration of the dry season in the arc of deforestation. Int. J. Climatol. 30, 1970–1979, http://dx.doi.org/10.1002/joc.2048.

Danelichen, V.H.M., Machado, N.G., Souza, M.C., Biudes, M.S., 2013. TRMM satellite performance in estimating rainfall over the Midwest region of Brazil. Rev. Bras. Climatol. 9 (2), 22–31.

da Rocha, H.R., Goulden, M.L., Miller, S.D., Menton, M.C., Pinto, L.D.V.O., Freitas, H.C., Figuera, A.M.S., 2004. Seasonality of water and heat fluxes over a tropical forest in eastern Amazonia. Ecol. Appl. 14, 22–32, http://dx.doi.org/10.1890/02-6001.

da Rocha, H.R., Manzi, A.O., Cabral, O.M., Miller, S.D., Goulden, M.L., Saleska, S.R., Coupe, N.R., Wofsy, S.C., Borma, L.S., Artaxo, P., Vourlitis, G., Nogueira, J.S., Cardoso, F.L., Nobre, A.D., Kruijt, B., Freitas, H.C., von Randow, C., Aguiar, R.G., Maia, J.F., 2009. Patterns of water and heat flux across a biome gradient from tropical forest to savanna in Brazil. J. Geophys. Res. 114 (G00B12), 1–8, http://dx.doi.org/10.1029/2007 JG000640.

Dalmagro, H.J., Lobo, F.A., Vourlitis, G.L., Dalmolin, Â.C., Antunes Jr., M.Z., Ortíz, C.E.R., Nogueira, J.S., 2014. The physiological light response of two tree species across a hydrologic gradient in Brazilian savanna (Cerrado). Photosynthetica 52, 22–35, http://dx.doi.org/10.1007/s11099-014-0001-5.

Dicken, U., Cohen, S., Tanny, J., 2013. Examination of the Bowen ratio energy balance technique for evapotranspiration estimates in screenhouses. Biosyst. Eng. 114, 397–405, http://dx.doi.org/10.1016/j.biosystemseng.2012.11.001.

Dirmeyer, P.A., 1994. Vegetation as a feedback mechanism in midlatitude drought. J. Clim. 7, 1463–1483, http://dx.doi.org/10.1175/1520-0442(1994)007<1463:VSAAFM>2.0.CO;2.

Domingues, A.N., de Abreu, J.G., Caneppele, C., dos Reis, R.H.P., Neto, A.B., de Almeida, C.M., 2013. Agronomic characteristics of corn hybrids for silage production in the State of Mato Grosso, Brazil. Acta Scientiarum 35 (1), 7–12, http://dx.doi.org/10.4025/actascianimsci.v35i1.15592.

Drexler, J.Z., Snyder, R.L., Spano, D., Paw, U.K.T., 2004. A review of models and micrometeorological methods used to estimate wetland evapotranspiration. Hydrol. Process. 18 (11), 2071–2101, http://dx.doi.org/10.1002/hyp.1462.

Dubreuil, V., Debortoli, N., Funatsu, B., Nédélec, V., Durieux, L., 2012. Impact of land-cover change in the Southern Amazonia climate: a case study for the region of Alta Floresta, Mato Grosso, Brazil. Environ. Monit. Assess. 184, 877–891, http://dx.doi.org/10.1007/s10661-011-2006-x.

Efron, B., Tibshirani, R., 1993. An Introduction to the Bootstrap. Chapman and Hall, New York.

Fausto, M.A., Machado, N.G., Nogueira, J.S., Biudes, M.S., 2014. Net radiation estimated by remote sensing in Cerrado áreas in the Upper Paraguay River Basin. J. Appl. Remote Sens. 8, 083541-1, http://dx.doi.org/10.1117/1.JRS.8.083541.

Fearnside, P.M., 2003. Deforestation control in Mato Grosso: a new model for slowing the loss of Brazil's Amazon forest. AMBIO 32 (5), 343–345, http://dx.doi.org/10.1579/0044-7447-32.5.343.

Fisch, G., Tota, J., Machado, A.T., Silva Dias, M.A.F., Lyra, R.F.F., Nobre, C.A., Dolman, A.J., Gash, J.H.C., 2004. The convective boundary layer over pasture and forest in Amazonia. Theor. Appl. Climatol. 78 (1–3), 47–59, http://dx.doi.org/10.1007/s00704-004-0043-x.

Fisher, R.A., Williams, M., da Costa, A.L., Malhi, Y., da Costa, R.F., Almeida, S., Meir, P.W., 2007. The response of an Eastern Amazonian rainforest to drought stress: results and modelling analyses from a through-fall exclusion experiment. Glob. Change Biol. 13, 1–8, http://dx.doi.org/10.1111/j.1365-2486.2007.01417.x.

Fisher, R.A., Williams, M., Ruivo, M.L., de Costa, A.L., Meir, P., 2008. Evaluating climatic and soil water controls on evapotranspiration at two Amazonian rainforest sites. Agric. For. Meteorol. 148, 850–861, http://dx.doi.org/10.1016/j.agrformet.2007.12.001.

Furley, P.A., Ratter, J.A., 1988. Soil resources and plant communities of the central Brazilian cerrado and their development. J. Biogeogr. 15, 97–108.

Galvão, L.S., Santos, J.R., Roberts, D.A., Breunig, F.M., Toomey, M., Moura, Y.M., 2011. On intra-annual EVI variability in the dry season of tropical forest: a case study with MODIS and hyperspectral data. Remote Sens. Environ. 115, 2350–2359, http://dx.doi.org/10.1016/j.rse.2011.04.035.

Garcia-Carreras, L., Parker, D.J., 2011. How does local tropical deforestation affect rainfall? Geophys. Res. Lett. 38, L19802, http://dx.doi.org/10.1029/2011 GL049099.

Ghil, M., Allen, M.R., Dettinger, M.D., Ide, K., Kondrashov, D., Mann, M.E., Robertson, A.W., Saunders, A., Tian, Y., Varadi, F., Yiou, P., 2002. Advanced Spectral Methods for Climatic Time Series. Rev. Geophys. 40 (1), 3.1–3.41, http://dx.doi.org/10.1029/2000RG000092.

Giambelluca, T.W., Scholz, F.G., Bucci, S.J., Meinzer, F.C., Goldstein, G., Hoffmann, W.A., Franco, A.C., Buchert, M.P., 2009. Evapotranspiration and energy balance of Brazilians savannas with contrasting tree density. Agric. For. Meteorol. 149, 1365–1376, http://dx.doi.org/10.1016/j.agrformet.2009.03.006.

Golyandina, N., Osipova, E., 2007. The 'Caterpillar' – SSA method for analysis of time series with missing values. J. Stat. Plan. Inference 137, 2642–2653, http://dx.doi.org/10.1016/j.jspi.2006.05.014.

Grace, J., Malhi, Y., Lloyd, J., Mcintyre, J., Miranda, A.C., Meir, P., Miranda, H.S., 1996. The use of eddy covariance to infer the net carbon dioxide uptake of Brazilian rain forest. Glob. Change Biol. 2, 209–217, http://dx.doi.org/10.1111/j.1365-2486.1996.tb00073.x.

Hasler, N., Avissar, R., 2007. What controls evapotranspiration in the Amazon Basin? J. Hydrometeorol. 8, 380–395, http://dx.doi.org/10.1175/JHM587.1.

Hernance, J.F., Jacob, R.W., Bradley, B.A., Mustard, J.F., 2007. Extracting phenological signals from multiyear AVHRR NDVI time series: framework for applying high-order annual splines. IEEE Trans. Geosci. Remote Sens. 45 (10), 3264–3276, http://dx.doi.org/10.1109/TGRS2007.903044.

Hilker, T., Lyapustin, A.I., Tucker, C.J., Sellers, P.J., Hall, F.G., Wang, Y., 2012. Remote sensing of tropical ecosystems: atmospheric correction and cloud masking matter. Remote Sens. Environ. 127, 370–384, http://dx.doi.org/10.1016/j.rse.2012.08.035.

Hird, J.N., McDermid, G.J., 2009. Noise reduction of NDVI time series: an empirical comparison of selected techniques. Remote Sens. Environ. 113, 248–258, http://dx.doi.org/10.1016/j.rse.2008.09.003.

Hu, S., Zhao, C., Li, J., Wang, F., Chen, Y., 2013. Discussion and reassessment of the method used for accepting or rejecting data observed by a Bowen ratio system. Hydrol. Process., http://dx.doi.org/10.1002/hyp.9962.

Huete, A.R., Restrepo-Coupe, N., Ratana, P., Didana, K., Saleskab, S.R., Ichiie, K., Panuthaif, S., Gamog, M., 2008. Multiple site tower flux and remote sensing comparisons of tropical forest dynamics in Monsoon Asia. Agric. For. Meteorol. 148, 748–760, http://dx.doi.org/10.1016/j.agrformet.2008.01.012.

Hutyra, L.R., Munger, J.W., Saleska, S.R., Gottlieb, E., Daube, B.C., Dunn, A.L., Amaral, D.F., de Camargo, P.B., Wofsy, S.C., 2007. Seasonal controls on the exchange of carbon and water in an Amazonian rain forest. J. Geophys. Res. 112, G03008, http://dx.doi.org/10.1029/2006JG000365.

Jasinski, E., Morton, D., DeFries, R., Shimabukuro, Y., Anderson, L., Hansen, M., 2005. Physical landscape correlates of the expansion of mechanized agriculture in Mato Grosso, Brazil. Earth Interact. 9, 1–18, http://dx.doi.org/10.1175/EI143.1.

Juárez, R.I.N., Hodnett, M.G., Fu, R., Goulden, M., von Randow, C., 2007. Control of dry season evapotranspiration over the Amazonian forest as inferred from observations at a southern Amazon forest site. J. Clim. 20, 2827–2839, http://dx.doi.org/10.1175/JCLI4184.1.

Li, W., Fu, R., Dickinson, R.E., 2006. Rainfall and its seasonality over the Amazon in the 21st century as assessed by the coupled models for the IPCC AR4. J. Geophys. Res. 111, D02111, http://dx.doi.org/10.1029/2005JD006355.

Li, W., Fu, R., Negron Juarez, R.I., Fernandes, K., 2008. Observed change of the standardized precipitation index, its potential cause and implications to future climate change in the Amazon region. Philos. Trans. R. Soc. B 363 (1498), 1767–1772, http://dx.doi.org/10.1098/rstb.2007.0022.

Li, Z., Barker, H., Moreau, L., 1995. The variable effect of clouds on atmospheric absorption of solar radiation. Nature 376, 486–490, http://dx.doi.org/10.1038/376486a0.

Lopes, A.S., Cox, F.R., 1977. Cerrado vegetation in Brazil: an edaphic gradient. Agric. J. 69, 828–831.

Machado, L.A.T., Laurent, H., Dessay, N., Miranda, I., 2004. Seasonal and diurnal variability of convection over the Amazonia: a comparison of different vegetation types and large scale forcing. Theor. Appl. Climatol. 78 (1–3), 61–77, http://dx.doi.org/10.1007/s00704-004-0044-9.

Machado, N.G., Sanches, L., Silva, L.B., Novais, J.W.Z., Aquino, A.M., Biudes, M.S., Pinto-Junior, O.B., Nogueira, J.S., 2015. Soil nutrients and vegetation structure in a neotropical seasonal wetland. Appl. Ecol. Environ. Res. 13 (2), 289–305, http://dx.doi.org/10.15666/aeer/1302_289305.

Malhi, Y., Wright, J., 2005. Late twentieth-century patterns and trends in the climate of tropical forest regions. In: Mahli, Y., Phillips, O.L. (Eds.), Tropical Forests and Global Atmospheric Change. Oxford University Press, Oxford, pp. 3–16.

Malhi, Y., Roberts, J.T., Betts, R.A., Killeen, T.J., Li, W., Nobre, C.A., 2008. Climate change, deforestation, and fate of the Amazon. Science 319 (5860), 169–172, http://dx.doi.org/10.1126/science.1146961.

Marengo, J.A., Tomasella, J., Alves, L.M., Soares, W.R., Rodriguez, D.A., 2011. The drought of 2010 in the context of historical droughts in the Amazon region. Geophys. Res. Lett. 38, L12703, http://dx.doi.org/10.1029/2011GL047436.

Moore, C.J., Fisch, G., 1986. Estimating heat storage in Amazonian tropical forest. Agric. For. Meteorol. 38 (1–3), 147–168, http://dx.doi.org/10.1016/0168-1923(86)90055-9.

Myneni, R.B., Yang, W.Z., Nemani, R.R., Huete, A.R., Dickinson, R.E., Knyazikhin, Y., Didan, K., Fu, R., Juárez, R.I.N., Saatchi, S.S., Hashimoto, H., Ichii, K., Shabanov, N.V., Tan, B., Ratana, P., Privette, J.L., Morisette, J.T., Vermote, E.F., Roy, D.P., Wolfe, R.E., Friedl, M.A., Running, S.W., Votava, P., El-Saleous, N., Devadiga, S., Su, Y., Salomonson, V.V., 2007. Large seasonal swings in leaf area of Amazon rainforests. Proc. Natl. Acad. Sci. U. S. A. 104, 4820–4823, http://dx.doi.org/10.1073/pnas.0611338104.

Nunes da Cunha, C., Junk, W.J., 2004. Year-to-year changes in water level drive the invasion of *Vochysia divergens* in Pantanal grasslands. Appl. Veg. Sci. 7 (1), 103–110, http://dx.doi.org/10.1111/j.1654-109X 2004.tb00600.x.

Ortega-Farias, S.O., Cuenca, R.H., Ek, M., 1996. Daytime variation of sensible heat flux estimated by the bulk aerodynamic method over a grass canopy. Agric. For. Meteorol. 81, 131–143, http://dx.doi.org/10.1016/0168-1923(95)02278-3.

Penha, J.M., da Silva, C.J., Bianchini, I., 1999. Productivity of the aquatic macrophytes *Pontederia lanceolata* Nutt. (Pontederiaceae) on the floodplains of the Pantanal Mato-grossense, Brazil. Wetl. Ecol. Manage. 7, 155–163, http://dx.doi.org/10.1023/A:1008463328612.

Perez, P.J., Castellvi, F., Ibanez, M., Rosell, J.I., 1999. Assessment of reliability of Bowen ratio method for partitioning fluxes. Agric. For. Meteorol. 97, 141–150, http://dx.doi.org/10.1016/S0168-1923(99)00080-5.

Pielke, R.A., 2001. Influence of the spatial distribution of vegetation and soils on the prediction of cumulus convective rainfall. Rev. Geophys. 39, 151–177, http://dx.doi.org/10.1029/1999RG000072.

Pongratz, J., Bounoua, L., DeFries, R.S., Morton, D.C., Anderson, L.O., Mauser, W., Klink, C.A., 2006. The impact of land cover change on surface energy and water balance in Mato Grosso, Brazil. Earth Interact. 10, 1–17, http://dx.doi.org/10.1175/EI176.1.

Priante-Filho, N., Vourlitis, G.L., Hayashi, M.M.S., Nogueira, J.S., Campelo, J.H., Nunes, P.C., Souza, L.S.E., Couto, E.G., Hoeger, W., Raiter, F., Trienweiler, J.L., Miranda, E.J., Priante, P.C., Fritzen, C.L., Lacerda, M., Pereira, L.C., Biudes, M.S., Suli, G.S., Shiraiwa, S., Paulo, S.R., Silveira, M., 2004. Comparison of the mass and energy exchange of a pasture and a mature transitional tropical forest of the Southern Amazon Basin during a seasonal transition. Glob. Change Biol. 10, 863–876, http://dx.doi.org/10.1111/j.1529-8817.2003.00775.x.

Quesada, C.A., Lloyd, J., Schwarz, M., Patiño, S., Baker, T.R., Czimczik, C., Fyllas, N.M., Martinelli, L., Nardoto, G.B., Schmerler, J., Santos, A.J.B., Hodnett, M.G., Herrera, R., Luizão, F.J., Arneth, A., Lloyd, G., Dezzeo, N., Hilke, I., Kuhlmann, I., Raessler, M., Brand, W.A., Geilmann, H., Moraes Filho, J.O., Carvalho, F.P., Araujo Filho, R.N., Chaves, J.E., Cruz Junior, O.F., Pimentel, T.P., Paiva, R., 2010. Variations in chemical and physical properties of Amazon forest soils in relation to their genesis. Biogeosciences 7, 1515–1541, http://dx.doi.org/10.5194/bg-7-1515-2010.

Radambrasil, 1982. Levantamentos dos Recursos Naturais Ministério das Minas de Energia. Secretaria Geral. Projeto RADAMBRASIL. Folha SD 21 Cuiabá, Rio de Janeiro, Brazil.

Ratana, T., Huete, A.R., Ferreira, L., 2005. Analysis of cerrado physiognomies and conversion in the MODIS seasonal–temporal domain. Earth Interact. 9 (3), 1–22, http://dx.doi.org/10.1175/1087-3562(2005)009<0001:AOCPAC>2.0.CO;2.

Reynolds, D.W., Haar, T.H.V., Cox, S.K., 1975. The effect of solar radiation absorption in the tropical troposphere. J. Appl. Meteorol. 14 (4), 433–444, http://dx.doi.org/10.1175/1520-0450(1975)014<0433:TEOSRA>2.0.CO;2.

Rodrigues, J.O., Andrade, E.M., Teixeira, A.S., Silva, B.B., 2009. Sazonalidade de variáveis biofísicas em regiões semiáridas pelo emprego do sensoriamento remoto. Engenharia Agrícola 29 (3), 452–465, http://dx.doi.org/10.1590/S0100-69162009000300012.

Rodrigues, T.R., de Paulo, S.R., Novais, J.W.Z., Curado, L.F.A., Nogueira, J.S., de Oliveira, R.G., Lobo, F.A., Vourlitis, G.L., 2013. Temporal patterns of energy balance for a Brazilian tropical savanna under contrasting seasonal conditions. Int. J. Atmos. Sci. 2013, 1–9, http://dx.doi.org/10.1155/2013/326010.

Rodrigues, T.R., Vourlitis, G.L., Lobo, F.A., Oliveira, R.G., Nogueira, J.S., 2014. Seasonal variation in energy balance and canopy conductance for a tropical savanna ecosystem of south central Mato Grosso, Brazil. J. Geophys. Res. Biogeosci., http://dx.doi.org/10.1002/2013JG002472.

Saleska, S., da Rocha, H., Kruijt, B., Nobre, A., 2009. Ecosystem carbon fluxes and Amazonian forest metabolism. In: Keller, M., Bustamante, M., Gash, J., Dias, P.S., Saleska, S., Da Rocha, H., Kruijt, B., Nobre, A. (Eds.), Amazonia and Global Change, Geophysical Monograph Series. AGU, Washington, DC, pp. 389–408.

Saleska, S.R., Miller, S.D., Matross, D.M., Goulden, M.L., Wofsy, S.C., da Rocha, H.R., de Camargo, P.B., Crill, P., Daube, B.C., de Freitas, H.C., Hutyra, L., Keller, M., Kirchhoff, V., Menton, M., Munger, J.W., Pyle, E.H., Rice, A.H., Silva, H., 2003. Carbon in Amazon forests: unexpected seasonal fluxes and disturbance-induced losses. Science 302, 1554–1557, http://dx.doi.org/10.1126/science.1091165.

San Jose, J.J., Nikonova, N., Bracho, R., 1998. Comparison of factors affecting the water transfer in a cultivated paleotropical grass (*Brachiaria decumbens* Stapf) field and a Neotropical savanna during the dry season of the Orinoco lowlands. J. Appl. Meteorol. 37, 509–522.

Santos, A.J.B., Quesada, C.A., da Silva, G.T., Maia, J.F., Miranda, H.S., Miranda, A.C., Lloyd, J., 2004. High rates of net ecosystem carbon assimilation by Brachiara pasture in the Brazilian Cerrado. Glob. Change Biol. 10, 877–885, http://dx.doi.org/10.1111/j.1529-8817.2003.00777.x.

Santos, C.A.C., Rao, T.V.R., Manzi, A.O., 2011. Net radiation estimation under pasture and forest in Rondônia, Brazil, with TM Landsat 5 images. Atmósfera 24 (4), 435–446.

Santos, S.A., da Cunha, C.N., Tomás, W., de Abreu, U.G.P., Arieira, J., 2006. Plantas Invasoras no Pantanal: Como Entender o Problema e Soluções de Manejo por Meio de Diagnóstico Participativo. Boletim de Pesquisa e Desenvolvimento 66, Embrapa Pantanal, Corumbá, MS, Brasil., pp. 45.

Santos, V.A., (Under graduation) 2005. Análise florística e estrutural de uma floresta ombrófila aberta primária no Parque Estadual Cristalino, Alta Floresta – MT, Brasil. Monograph. Fundação Universidade do estado de Mato Grosso, Campus Universitário de Alta Floresta, Departamento de Engenharia Florestal.

Seth, A., Giorgi, F., 1996. Three-dimensional model study of organized mesoscale circulations induced by vegetation. J. Geophys. Res. 101 (D3), 7371–7391, http://dx.doi.org/10.1029/95JD02677.

Sheil, D., Murdiyarso, D., 2009. How forests attract rain: an examination of a new hypothesis. BioScience 59 (4), 341347, http://dx.doi.org/10.1525/bio.2009.59.4.12.

Snyder, P.K., 2010. The influence of tropical deforestation on the northern hemisphere climate by atmospheric teleconnections. Earth Interact. 14, 1–34, http://dx.doi.org/10.1175/2010EI280.1.

Soares-Filho, B.S., Nepstad, D.C., Curran, L.M., Cerqueira, G.C., Garcia, R.A., Ramos, C.A., Voll, E., McDonald, A., Lefebvre, P., Schlesinger, P., 2006. Modelling conservation in the Amazon Basin. Nature 440, 520–523, http://dx.doi.org/10.1038/nature04389.

Souza, M.C., Biudes, M.S., Danelichen, V.H.M., Machado, N.G., de Musis, C.R., Vourlitis, G.L., Nogueira, J.S., 2014. Estimation of gross primary production of the Amazon-Cerrado transitional forest by remote sensing techniques. Rev. Bras. Meteorol. 29 (1), 1–12, http://dx.doi.org/10.1590/S0102-77862014000100001.

Teepe, R., Dilling, H., Beese, F., 2003. Estimating water retention curves of forest soils from soil texture and bulk density. J. Plant Nutr. Soil Sci. 166, 111–119, http://dx.doi.org/10.1002/jpln.200390001.

Unland, H.E., Houser, P.R., Shuttleworth, W.J., Yang, Z.L., 1996. Surface flux measurement and modelling at a semi-arid Sonoran Desert site. Agric. For. Meteorol. 82, 119–153, http://dx.doi.org/10.1016/0168-1923(96)02330-1.

Vermote, E.F., Kotchenova, S., 2008. Atmospheric correction for the monitoring of land surfaces. J. Geophys. Res. Atmos. 113 (D23), D23S90, http://dx.doi.org/10.1029/2007JD009662.

von Randow, C., Manzi, A.O., Kruijt, B., de Oliveira, P.J., Zanchi, F.B., Silva, R.L., Hodnett, M.G., Gash, J.H.C., Elbers, J.A., Waterloo, M.J., Cardoso, F.L., Kabat, P., 2004. Comparative measurements and seasonal variations in energy and carbon exchange over forest and pasture in South West Amazonia. Theor. Appl. Climatol. 78 (1–3), 5–26, http://dx.doi.org/10.1007/s00704-004-0041-z.

Vourlitis, G.L., da Rocha, H.R., 2011. Flux dynamics in the cerrado and cerrado-forest transition of Brazil. In: Hill, M.J., Hanan, N.P. (Eds.), Ecosystem Function in Global Savannas: Measurement and Modeling at Landscape to Global Scales. CRC Inc., Boca Raton, FL, USA.

Vourlitis, G.L., Lobo, F.A., Biudes, M.S., Ortíz, C.E.R., Nogueira, J.S., 2011. Spatial variations in soil chemistry and organic matter content across a Vochysia divergens invasion front in the Brazilian Pantanal. Soil Sci. Soc. Am. J. 75 (4), 1554–1561, http://dx.doi.org/10.2136/sssaj2010.0412.

Vourlitis, G.L., Lobo, F.A., Lawrence, S., Lucena, I.C., Borges Jr., O.B., Dalmagro, H.J., Ortiz, C.E.R., Nogueira, J.S., 2013. Variations in stand structure and diversity along a soil fertility gradient in a Brazilian savanna (Cerrado) in southern Mato Grosso. Soil Sci. Soc. Am. J. 77, 1370–1379, http://dx.doi.org/10.2136/sssaj2012.0336.

Vourlitis, G.L., Nogueira, J.S., Lobo, F.A., Pinto Jr., O.B., 2014. Variations in evapotranspiration and climate for an Amazonian semi-deciduous forest over seasonal, annual, and El Niño cycles. Int. J. Biometeorol., http://dx.doi.org/10.1007/s00484-014-0837-1.

Vourlitis, G.L., Nogueira, J.S., Lobo, F.A., Sendall, K.M., de Faria, J.L.B., Dias, C.A.A., Andrade, N.L.R., 2008. Energy balance and canopy conductance of a tropical semi-deciduous forest of the Southern Amazon Basin. Water Resour. Res. 44 (3), W03412, http://dx.doi.org/10.1029/2006 WR005526.

Vourlitis, G.L., Priante-Filho, N., Hayashi, M.M.S., Nogueira, J.S., Caseiro, F.T., Campelo Junior, J.H., 2002. Seasonal variations in the evapotranspiration of a transitional tropical forest of Mato Grosso, Brazil. Water Resour. Res. 38 (6), 1094, http://dx.doi.org/10.1029/2000WR000122.

Werth, D., Avissar, R., 2002. The local and global effects of Amazon deforestation. J. Geophys. Res. 107 (D20), 8087, http://dx.doi.org/10.1029/2001JD000717.

Werth, D., Avissar, R., 2004. The regional evapotranspiration of the Amazon. J. Hydrometeorol. 5, 100–109, http://dx.doi.org/10.1175/1525-7541(2004)005<0100:TREOTA>2.0.CO;2.

Xiao, X., Hagen, S., Zhang, Q., Keller, M., Moore, B., 2006. Detecting leaf phenology of seasonally moist tropical forests in South America with multi-temporal modis images. Remote Sens. Environ. 103, 465–473, http://dx.doi.org/10.1016/j.rse.2006.04.013.

Zeilhofer, P., 2006. Soil mapping in the Pantanal of Mato Grosso, Brazil using multitemporal Landsat TM data. Wetl. Ecol. Manage. 14 (5), 445–461, http://dx.doi.org/10.1007/s11273-006-0007-2.

Zhang, X., Friedl, M.A., Schaaf, C.B., 2006. Global vegetation phenology from Moderate Resolution Imaging Spectroradiometer (MODIS). J. Geophys. Res. 111, G04017, http://dx.doi.org/10.1029/2006JG000217.